Quantitative Mapping of Regional Cerebral Blood Flow Using Iodine-123-IMP and SPECT

Hidehiro Iida, Hiroshi Itoh, Mayumi Nakazawa, Jun Hatazawa, Hiromi Nishimura, Yoshihiro Onishi and Kazuo Uemura

Research Institute for Brain and Blood Vessels, Akita; Institute for Cancer and Tuberculosis, Tohoku University, Miyagi; and Nihon Medi-Physics, Hyogo, Japan

A method was developed to calculate functional images of regional cerebral blood flow (rCBF) from a single scan using SPECT following intravenous ^{123}I-N-isopropyl-p-iodoamphetamine (IMP) infusion. **Methods:** A two-compartment model that includes two parameters of rCBF and regional distribution volume of IMP (V_d) was employed to correct for clearance of IMP from the brain. Using a given input function and a fixed V_d value (30 ml/ml according to an analysis on dynamic SPECT data), a unique value of rCBF was calculated for each pixel of the SPECT image according to the table-look-up procedure. This technique was applied to 15 human subjects, and the calculated rCBF values were compared with those measured by PET. **Results:** A set of simulation studies demonstrated an optimal SPECT midscan time at 30 to 40 min postinjection of IMP, providing the minimal error sensitivity to the individual difference of the input function (rCBF values with an accuracy of ±10%). Another set of simulation suggested validity of fixing the V_d values, i.e., errors in calculated rCBF values were around ±7% for a change of V_d of ±10%. The measured rCBF values obtained from 15 human subjects were independent on the SPECT scan time. The calculated rCBF values also agreed well with those obtained by the nonlinear least-squares fitting analysis that were obtained from the dynamic SPECT scan and the frequent arterial blood sampling and measurement of lipophilic fraction for each sample ($0.54 + 0.88x$, $r = 0.86$), suggesting the validity of the simplified procedures in this method. **Conclusion:** These observations suggested the validity of this method as a clinical tool for quantitative measurement of rCBF.

Key Words: iodine-123-IMP; regional cerebral blood flow; SPECT

J Nucl Med 1994; 35:2019–2030

Iodine-123-N-isopropyl-p-iodoamphetamine (IMP) is used for mapping brain perfusion with SPECT (*1–3*). Because of its relatively high first-pass extraction fraction and high affinity in the brain, the early picture following the intravenous administration of IMP reflects the distribution of regional cerebral blood flow (rCBF); with arterial blood sampling (e.g., continuous arterial withdrawal during the early period), absolute quantification of the rCBF value is possible (*2*). However, as has been demonstrated by several investigators, IMP has significant clearance from the brain (*4–8*), and this can cause a systematic underestimation of the global CBF values and reduction in contrast between high rCBF and low rCBF regions (*9,10*). To avoid the effects of the clearance, acquisition of the SPECT data at extremely early period (e.g., less than 5 min) was suggested (*2,9,10*). This, however, would be of a limited applicability in a clinical study, particularly when using a conventional rotating gamma camera, because of the limited accuracy of the SPECT data being acquired when the radioactivity distribution varies (*2*).

On the other hand, recent studies revealed that the IMP kinetics in the brain follow the two-compartment model (*10–12*). Values of rCBF can then be calculated based on nonlinear least-squares fitting (NLLSF) (*2,6*) or other techniques (*10–12*). These techniques, however, required too laborious procedures, including sequential data acquisition by a dynamic SPECT scan following the IMP infusion, frequent arterial blood sampling and separation of the lypophilic fractions for each blood sample. Thus, they have limited application for clinical use.

The purpose of this study was to develop a new clinical method to calculate a quantitative rCBF map using IMP and SPECT. For the method to be clinical, the authors intended to minimize the procedures required for the quantitative calculation. The clearance of IMP from the brain was corrected by assuming a fixed regional distribution volume (a parameter associated with the clearance rate in the two-compartment model), and its validity was investigated. The frequent arterial blood sampling (or the continuous blood sampling during the early period) was avoided by employing a standardized input function derived from an independent study population. The whole-blood radioactivity of a single blood sample was referred to calibrate this standard input function. To minimize errors caused by the interindividual difference of the input function, timing of the SPECT scan and that of the blood sample were optimized. Finally, the accuracy of this method was evaluated by comparing it with an independent technique using PET.

Received Dec. 1, 1993; revision accepted Aug. 22, 1994.

For correspondence or reprints contact: Dr. Hidehiro Iida, DSc, Department of Radiology and Nuclear Medicine, Research Institute for Brain and Blood Vessels, Senshu-kubota machi, Akita City, Akita, Japan 010.

THEORY

Kinetics of IMP

To describe the kinetics of IMP in the brain, the two-compartment model was employed in this study according to the previous reports (*2,6,9–12*). Using this model, the radioactivity concentration in the brain at time t, i.e., $C_t(t)$ (in MBq/ml), is given by:

$$C_t(t) = K_1 \cdot C_a(t) \otimes e^{-k_2 \cdot t}, \qquad \text{Eq. 1}$$

where $C_a(t)$ is the arterial input function, $\otimes$ is the convolution integral, and K_1 (in ml blood/min/ml of a given volume element) and k_2 (in reciprocal min) denote the influx and outflux rates of IMP through the capillary membrane, respectively. K_1 and k_2 have following relations to rCBF (f):

$$K_1 = \rho \cdot E \cdot f, \qquad \text{Eq. 2a}$$

$$k_2 = \frac{f}{\lambda}, \qquad \text{Eq. 2b}$$

where ρ is the density of the brain tissue (assumed to be 1.04 g of tissue per ml of a given volume element in this study), E is the first-pass extraction fraction (assumed to be 1.0), f (in ml blood/min/g of tissue) is rCBF, and λ (in g/ml) is the regional partition coefficient of IMP. The regional distribution volume (V_d) of IMP is defined as a ratio of the influx to the outflux rates (K_1/k_2), and thus

$$V_d = \rho \cdot \lambda \qquad \text{Eq. 3}$$

Inserting Equations 2a, 2b and 3 into Equation 1 and assuming

E = 1.0 provide:

$$C_t(t) = \rho \cdot f \cdot C_a(t) \otimes e^{-(\rho \cdot f/V_d) \cdot t}. \qquad \text{Eq. 4}$$

Thus, for a given SPECT scan time (midscan time, MST = t), a given value of V_d and a given input function [$C_a(t)$] together with an assumed ρ value, Equation 4 provides a unique relation between $C_t(t)$ and rCBF (f).

Calculation of rCBF from a Single SPECT Scan

Functional images of rCBF are calculated from a single SPECT scan data obtained after the IMP administration (IMP autoradiography [ARG]). First, a table of $C_t(t)$ on the right side of Equation 4 is calculated as a function of rCBF (f). For a given input function, $C_a(t)$, a given SPECT MST (t) and a given value of V_d, this calculation is done only once. Second, a value for f (rCBF) is obtained through the table-look-up procedure using the calculated table from the SPECT image taken at MST of t. A standard input function is used in this study, and a single arterial blood sample taken at t = 9 min is referenced to the standardized input function to obtain the individual arterial input function, $C_a(t)$ (discussed later).

Calculation of rCBF by Nonlinear Least-Squares Fitting

To validate the method described earlier (IMP ARG method), values of rCBF are also calculated using a conventional NLLSF technique. Two parameters of f (rCBF) and V_d are fitted so that the predicted time-activity curve (Equation 4) best reproduces the measured time-activity curve. The regional time-activity curve is measured by a dynamic SPECT scan following IMP administration. This calculation is done only for a given region of interest (ROI). The arterial input function is obtained from the frequent arterial blood sampling in each study (measurements of the whole-blood radioactivity concentrations and their lipophilic fractions for all samples discussed later).

METHODS

Standard Input Function

The standard input function was obtained following IMP administration in the 12 subjects (exclusive to the subject group that underwent the SPECT study). The subjects consisted of eight male normal volunteers and four patients with chronic cerebral infarction. Ages ranged from 31 to 72 yr (average 55 yr). None of them showed any abnormality in their lung or cardiac functions. Five were smokers. A 222-MBq dose of IMP (111 MBq in four cases, with the input data scaled to equivalent to the 222-MBq dose) was infused into the antecubital vein continuously at a constant infusion rate for a period of 1.0 min. Following the infusion start, arterial blood (approximately 1.5 ml) was sampled frequently from the radial artery. The withdrawal time was less than 2 sec for all samples. The samples were taken every 15 sec for the first 2 min, and the interval was gradually prolonged until 90 min. For all blood samples, the whole-blood radioactivity concentrations (in cps/g) and their octanol extraction fractions (lipophilic fraction) were measured (*2*). The standard input function was obtained as the numerical average of the 12 individual input functions derived by multiplying the whole blood radioactivity concentration by the octanol extraction fraction for each sample.

The optimal time to calibrate the standard input function in the individual study was determined to minimize the difference of integration (from 0 to 40 min) of the calibrated standard input function from that of the true input function measured in each of the 12 studies. The following cost function $\Omega(T_c)$ is minimized for this estimate:

$$\Omega(T_c) = \frac{1}{12} \cdot \sum_{i=1}^{12} \frac{\left| \int_0^{T = 40\ \text{min}} C_a^i(s)\, ds - \int_0^{T = 40\ \text{min}} \phi(T_c) \cdot A(s)\, ds \right|}{\int_0^{T = 40\ \text{min}} C_a^i(s)\, ds}, \qquad \text{Eq. 5}$$

where $\phi(T_c)$ denotes the calibration factor calculated as a ratio of whole-blood counts at time t (a ratio of the whole-blood counts in each subject to that in the standard whole blood curve), $C_a^i(t)$ is the individual input function (whole-blood radioactivity × octanol extraction fraction) of the ith subject, A(t) is the standard input function, and T (= 40 min) is the integration period for the two input functions. Minimization of this cost function yields an optimal calibration time (i.e., the optimal blood sampling time), which maximizes the accuracy of integration of the calibrated, standard arterial input function.

Simulation

Relationship Between SPECT Counts and rCBF. Regional radioactivity concentration in the brain was calculated as a function of rCBF for different V_d values and different MSTs using Equation 4. The standard input function described earlier was used in this calculation.

Error Sensitivity to V_d. A simulation study was performed to investigate effects of errors associated with the fixation of the V_d value. First, tissue radioactivity concentrations were simulated for various rCBF and V_d values using Equation 4. Second, rCBF values were calculated according to the IMP ARG method using a fixed value of V_d (30 ml/ml). Then, the percent error in rCBF (difference of the estimated rCBF from assumed rCBF values) was estimated as a function of true V_d values. This simulation was performed for the MSTs of 25, 30 and 40 min.

Effects of Individual Difference of Input Function. Another set of simulation studies was performed to investigate errors caused by the individual difference of the input function. First, regional brain radioactivity concentrations were generated according to Equation 4 for various MSTs using 12 input functions (original data for generating the standard input function). With these tissue concentrations, rCBF values were calculated according to the IMP ARG method, in which the standardized input function was employed. The whole-blood radioactivity concentration at 9 min post-IMP administration of each input function was used to calibrate the standard input function in each calculation. The s.d. in the calculated rCBF values was then estimated as a function of the SPECT MST for various rCBF values. The value of V_d was assumed to be 30 ml/ml in this simulation.

Error Sensitivity to SPECT Data. A simulation study was also performed to investigate the error sensitivity to the SPECT data. Tissue radioactivity concentration time-activity curves were simulated for rCBF = 20, 50 and 70 ml/min/g and V_d = 30 ml/ml using Equation 4. By the addition of an offset to the tissue concentration, rCBF values were calculated according to the IMP ARG method. Then, the percent error in rCBF (difference of the estimated rCBF from assumed rCBF values) was estimated as a function of the percent change of the tissue radioactivity concentration. This simulation was performed for MST of 40 min.

Subjects

SPECT studies were performed on 15 subjects, including two male normal volunteers (ages 26 and 44 yr), 12 patients with cerebrovascular disease (age range 44–74 yr, 9 male and 3 female) and one female patient with hypertension (age 66 yr). None of these subjects belonged to the study group for generating the standard input function described earlier. All subjects gave written informed consent to a protocol approved by the committee for the clinical research of this institute. These subjects were divided into two groups; the first group (5 subjects) had a dynamic SPECT scan with frequent arterial sampling, and the second group (10 subjects) underwent only a single SPECT scan with one arterial blood sampling (approximately at 9 min post-IMP administration).

The first group consisted of one male volunteer (age 26 yr) and four patients with cerebral infarction (age range 63–71 yr, three male and one female). Two patients had chronic cerebral infarction and other two, acute cerebral infarction (day 8 and 6). One patient with an acute infarction had showed chronic heart failure (NYHA grade 3) at the time of the SPECT scan. None of them were smokers or showed abnormalities in their lungs.

The second group included one male volunteer (age 44 yr) and nine patients. Four patients had chronic cerebral infarctions, two from myotonic dystrophy, one from chronic putaminal hemorrhage, one from carotid artery stenosis and another one from hypertension. Four subjects were smokers, but no one showed abnormalities in their lungs.

Dynamic SPECT Scan (Group 1)

Following a 1-min infusion of 222 MBq of IMP (same protocol used in the standard input function), a dynamic SPECT scan was obtained from five subjects. The scan sequence was ten 2-min, ten 4-min and three 10-min scans. The total scan time was 90 min. Frequent arterial blood sampling was performed in this group, and both the whole-blood radioactivity concentrations and the octanol extraction fractions were measured for each sample. Two kinds of input functions were determined for this group: (1) the true input function calculated by multiplying the whole-blood radioactivity concentration curve by the octanol extraction fraction in each sample and (2) an input function derived from the standard input function scaled by a factor determined by the blood sample taken at 9 min after the infusion start. Additional blood samples were taken at 5, 10, 20 and 60 min after the infusion start to measure the partial pressure of CO_2 in the arterial blood.

The SPECT scanner used for this group was Headtome-II [Shimadzu Corp., Kyoto, Japan (*13,14*)], which has three detector rings with 64 NaI rectangular detectors. The spatial resolution at the center of field of view (FOV) was 8 mm full width at half maximum (FWHM), and the slice thickness was 17 mm FWHM. Three tomographic images were taken at 7, 42 and 77 mm above and parallel to the orbital meatal (OM) line. The images were reconstructed using filtered back projection with a Butterworth filter. The attenuation correction was performed by assuming an elliptical brain outline.

Autoradiographic SPECT Scan (Group 2)

An additional 10 subjects (the second group) underwent the single-scan SPECT study using a Headtome-SET080 tomograph (Shimadzu), which provides 31 tomographic images. The data acquisition initiated at 30 min after the IMP administration for a scan duration of 20 min (MST = 40 min). A single blood sample was obtained from the brachial artery (t = 9–11 min post-IMP administration), and the whole-blood radioactivity concentration was measured to scale the standard input function. The spatial resolution of this scanner was 13 mm FWHM at the center of FOV, and the slice thickness was 25 mm FWHM at the center of FOV. Image slices were taken at 5-mm intervals parallel to the OM line. The images were reconstructed using the weighted-filtered back projection technique (*15*), in which the attenuation correction was made by detecting the edge of the object.

Cross Calibration

A cylindrical uniform phantom (16-cm inner diameter and 15-cm length) was used to calibrate the sensitivity of the SPECT scanner against a well counter system. Approximately 40 MBq of IMP was stirred in the phantom, and a SPECT scan was initiated for 10 min. A sample was taken from the phantom after the SPECT scan, and its radioactivity concentration was measured using a well counter. This cross calibration scan was performed twice before and after this SPECT study (an interval of approximately 3 wk). The calibration factor appeared to be consistent between the two studies, and the difference between the two studies was within 3% for all slices.

PET

To validate the method presented in this article (the IMP ARG method), all subjects had PET studies on the same day as the

SPECT study and approximately 1 hr before IMP administration. After a transmission scan for attenuation correction, a 90-sec scan was initiated following a bolus injection of ^{15}O-water ($H_2^{15}O$). The PET scanner used was the Headtome-IV (Shimadzu) (*16*) (seven-slice machine), which provides 14 tomographic images with 6.5-mm intervals by the continuous axial motion of the gantry. The image slices were parallel to the OM line (same as for the SPECT studies). The functional rCBF images were calculated according to the ^{15}O-water autoradiography (*17–21*). The distribution volume of water was assumed to be 0.80 ml/ml, which empirically corrects for the tissue heterogeneity and provides rCBF values that are independent of the scan period (*22,23*). The arterial input function was monitored continuously using a beta probe, and its delay and dispersion were corrected carefully according to the authors' previous report (*19–21*).

Data Analysis

All reconstructed image data (both SPECT and PET) were transferred to a conventional UNIX workstation (TITAN-750, Kubota Computer Corp., Tokyo, Japan), and all further analyses were done on this computer. SPECT images were corrected for the radioactive decay of ^{123}I back to the IMP injection start time, normalized by the data collection time and cross calibrated to the well counter system. In addition, images obtained from the first group were accumulated to provide six static images at the MSTs of 10, 20, 30, 40, 50 and 60 min (integration period was 8 min for each). The rCBF images were calculated according to the IMP ARG method for these accumulated images. The calculation of rCBF was also performed for the static SPECT images obtained from the second group. The whole-blood radioactivity counts of the single blood sample was refered to the standard input function in the calculation for both groups. The V_d value was assumed to be 30 ml/ml.

ROIs were drawn on both SPECT and PET images by an experienced radiologist. For the first group (n = 5), ROIs were relatively small and covered 10 regions of cortical gray matter, including territories of the anterior carotid artery, anterior trunk of the middle carotid artery (MCA), middle trunk of MCA, posterior trunk of MCA and posterior carotid artery. These ROIs included both normal and the low-density regions as defined by the x-ray CT. Elliptical ROIs with diameters of 16 mm in the short-axis and 32 to 64 mm in the long-axis were used. These ROIs were projected onto the dynamic SPECT images to provide the time-activity curves. For the second group, two large ROIs were manually selected in each subject. One ROI covered the whole tomographic slice at 40 mm above the OM line that includes the basal ganglia, the thalamus and the whole cerebellum. For both groups, ROIs were also selected on PET images with the same size and shape, and rCBF values were compared for each ROI.

For time-activity curves generated from the dynamic SPECT data (the first group), NLLSF analysis was performed to fit two parameters of f (rCBF) and V_d to the two-compartment model (Eq. 4). The individually measured input function was used in this calculation.

RESULTS

The 12 individual input functions and the combined, standard input function are shown in Figure 1. The data were obtained as a numerical product of the whole-blood radioactivity concentration and the octanol extraction fraction for each sample. The standard input function shown in Table 1 is calculated as the average of the 12 individual curves.

The s.d. of the cost function defined by Equation 5 (difference of the integration for the first 40 min) is shown in Table 2 as a function of the calibration time (T_c). Integration of the input functions was relatively stable, particularly when calibrated at a suitable time point, despite the individual variation of the shape particularly around the peak (Fig. 1). The minimum deviation of the cost function (5.3%) was obtained when the standard input function was calibrated at 9 min postadministration of IMP. The cost function increased gradually when the calibration time was delayed after 10 min and increased quite rapidly for calibration times earlier than 8 min.

Figure 2 shows the relationship between the regional brain radioactivity (SPECT counts) and rCBF for different combinations of the V_d and MST. The SPECT counts were monotonically increased as rCBF increased for the three conditions. It can be seen that the linearity at high rCBF is declined for the smaller V_d and delayed MST.

Figure 3 shows the results of a simulation study, demonstrating errors in the rCBF estimates caused by ambiguity of the assumed V_d value for MSTs of 25, 30 and 40 min. Larger errors are shown for the delayed MST. Errors in rCBF also become large for extremely high CBF. A change of V_d of ± 10% (i.e., V_d = 30 ± 3 ml/ml) corresponds to errors in rCBF of approximately ± 10% (4%) for MST of 40 min, ± 7% (3%) for MST of 30 min and ± 5% (2%) for MST of 25 min at rCBF = 50 ml/min/100 g (20 ml/min/100 g), respectively.

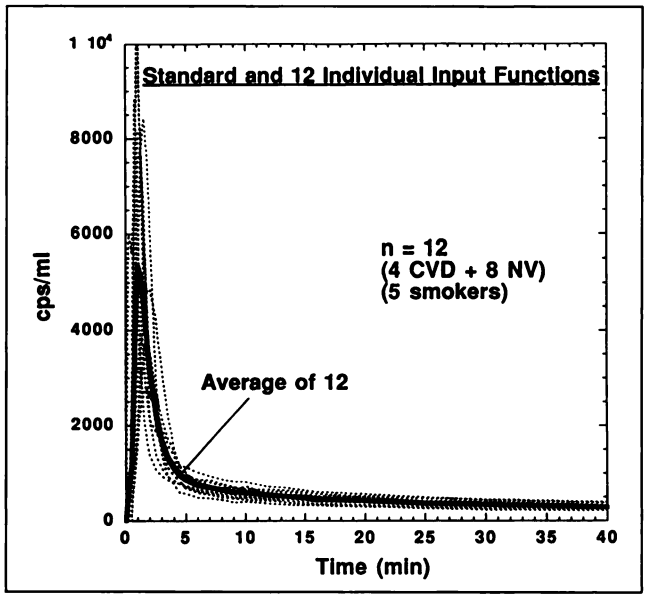

FIGURE 1. Arterial input functions obtained from 12 subjects by sequentially sampling the arterial blood following IMP administration (dotted lines). The data were calculated by multiplying the whole-blood radioactivity concentration by the octanol extraction fraction for each blood sample. The bold solid line corresponds to the standard input function and obtained as the average of 12 input functions.

Figure 4 shows results of the simulation study which demonstrate effects of individual difference of the standard input function on the rCBF estimates in the IMP ARG method. The s.d. of the calculated rCBF values were plotted as a function of SPECT MST. The s.d. of the calculated rCBF values was dependent on the rCBF value to be calculated (the error becomes larger at a high rCBF range). The optimal MST that gives the minimum s.d. in rCBF was slightly dependent on rCBF values to be calculated. The minimum error of 10% in rCBF corresponded to MST of 20 to 40 min for rCBF of 50 ml/min/100 g.

The results of the simulation study that demonstrates effects of errors in the SPECT data on the calculated rCBF values are shown in Figure 5. The error sensitivity to the SPECT data was found to be approximately 1.5 (i.e., a 10% error in the SPECT data corresponded to a 15% error in the calculated rCBF) for rCBF of 50 ml/min/100 g at the MST of 40 min. The error sensitivity was large for high rCBF but small for low rCBF.

NLLSF analysis for the dynamic SPECT data (the first group, n = 5) yielded rCBF and V_d values (average ± 1 s.d. for all ROIs) of 29.0 ± 12.0 ml/min/100 g and 30.1 ± 7.2 ml/ml, respectively. Both rCBF and V_d were significantly different between regions that showed normal density and low density in x-ray CT, i.e., rCBF of 31.3 ± 10.4 ml/min/

TABLE 1
Whole-Blood Radioactivity Curve [$C_{whole\text{-}blood}(t)$], Octanol Extraction Fraction [$E_{octanol}(t)$] and the Standard Input Function [$C_a(t)$]* Obtained from Averaging 12 Individual Input Functions

Time (min)	$C_{whole\text{-}blood}(t)$	$E_{octanol}(t)$	$C_a(t)$
0.25	680	0.782	532
0.5	1356	0.817	1108
0.75	4097	0.818	3350
1	6484	0.838	5434
1.25	6808	0.822	5600
1.5	6362	0.791	5030
1.75	5745	0.807	4611
2	4899	0.782	3833
2.5	3549	0.784	2784
3	2612	0.766	2002
3.5	2035	0.752	1531
4	1682	0.742	1249
4.5	1417	0.726	1029
5	1265	0.736	931
6	1085	0.719	780
7	996	0.703	700
8	931	0.716	667
9	870	0.717	624
10	828	0.706	585
12	761	0.705	537
14	714	0.702	501
16	645	0.695	448
20	601	0.700	421
25	525	0.683	358
30	480	0.670	322
40	399	0.650	259
50	364	0.645	235
60	320	0.608	195
70	300	0.590	177
80	280	0.609	171

*[$C_a(t)$] is calculated by multiplying $C_{whole\text{-}blood}(t)$ by $E_{octanol}(t)$ at each time point.

TABLE 2
Calibration Time to Scale the Standard Input Function (T_c) and Percent S.D. of the Cost Function Defined by Equation 5 $\Omega(T_c)$*

Calibration time (min)	% s.d. of $\Omega(T_c)$† (%)
2	42
3	33
4	20
5	8.6
6	6.6
7	5.9
8	5.4
9	5.3(minimum)
10	5.8
12	6.3
14	6.5
16	6.7
20	6.8
30	8.0
40	9.1
50	9.5
60	10.0

*Percent difference of integration for the first 40 min of the calibrated, standard input function from individual input functions.
†% s.d. of $\Omega(T_c)$ was minimum at T_c = 9 min.

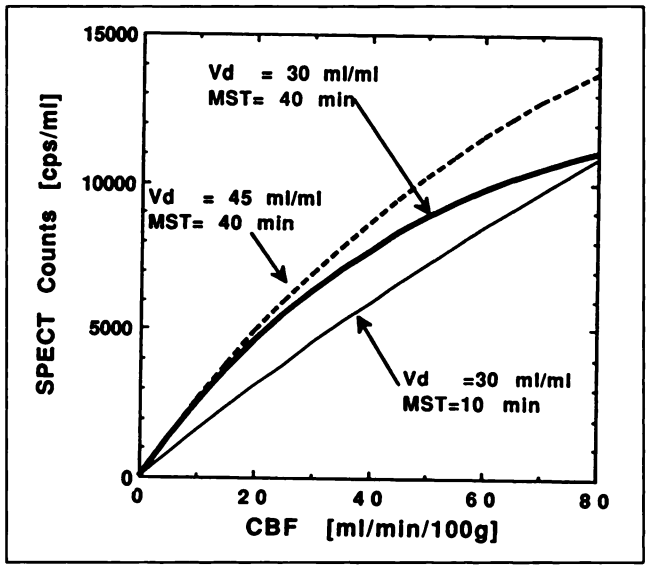

FIGURE 2. Simulated tissue radioactivity concentrations in the brain (SPECT counts) as a function of rCBF. Data are calculated according to the two-compartment model described in Equation 4. The bold solid line corresponds to V_d = 30 ml/ml and MST = 40 min, the line to V_d = 30 ml/ml and MST = 10 min and the dashed line to V_d = 45 ml/ml and MST = 40 min, respectively. Delayed MST and small V_d values provide declined linearity between the SPECT counts and rCBF, particularly at a high rCBF range.

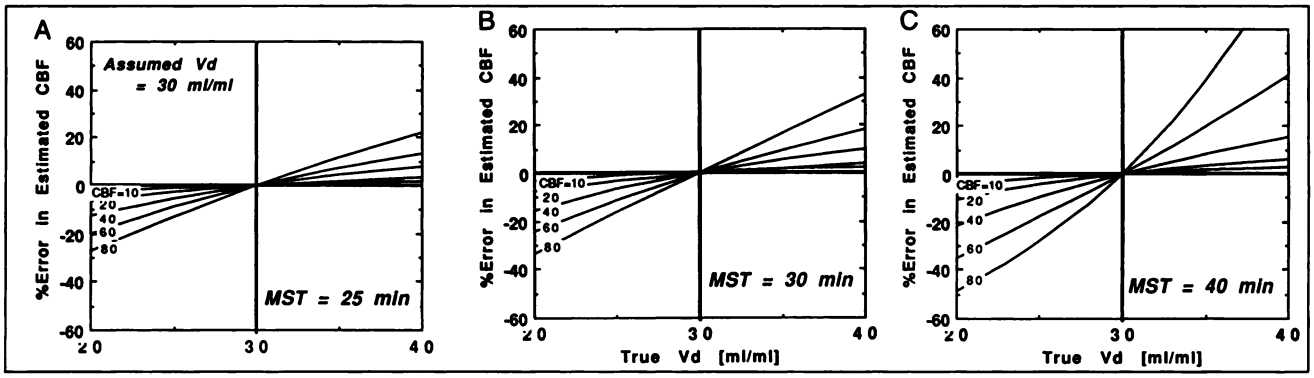

FIGURE 3. Results of a simulation study that demonstrates effects of fixation of the V_d value on the rCBF calculation in the IMP ARG method. Errors in the calculated rCBF values are plotted as a function of the true V_d values for various rCBFs (V_d = 30 ml/ml is assumed). (A) MST at 40 min post-IMP administration. (B) MST at 30 min. (C) MST at 25 min. Errors in rCBF increases at a high rCBF range, particularly for delayed MST.

100 g compared with 8.7 ± 4.2 ml/min/100 g and V_d of 31.5 ± 3.0 ml/ml compared with 10.1 ± 4.9 ml/ml corresponding to the normal and low-density regions, respectively (Table 3).

Original SPECT images and calculated rCBF images obtained from one of the first groups are compared in Figure 6 for various MSTs (i.e., 10, 20, 40, 60 and 80 min post-IMP administration). In this calculation, V_d = 30 ml/ml was assumed, and the standard input function was calibrated by using the whole-blood radioactivity concentration of the blood sample taken at 9 min post-IMP administration. It can be seen that the absolute magnitude of the original IMP images was highly dependent on the MST because the MST was delayed. On the other hand, the rCBF images calculated by the IMP ARG method were almost constant. It can also be seen that the contrast of the individual images between high and low count areas was significantly higher in the calculated rCBF images than the original images. Figure 7 shows another representative rCBF image for three tomographic slices calculated by the IMP ARG method (using the standard input function with one blood sample), with those obtained by the ^{15}O-water PET method demonstrating a reasonable agreement between the two rCBF images. The total image processing time to calculate the functional rCBF images was less than 1 sec using the TITAN-750 UNIX workstation. The com-

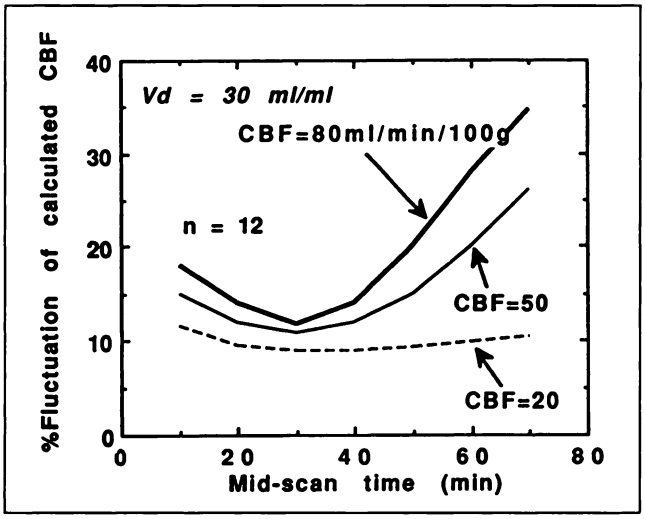

FIGURE 4. Results of a simulation study demonstrating effects of individual difference of the arterial input function on s.d. in rCBF estimates. Tissue radioactivity concentrations were generated using 12 individual input functions, and rCBF values were estimated by referring the standard input function and the radioactivity concentration at t = 9 min in each input function. Then, the s.d. of the difference in calculated rCBF values was plotted as a function of the SPECT MST. It can be seen that errors are dependent on the rCBF value to be estimated and vary dependent on MST. The minimum error of 10% in rCBF corresponded to MST of 20 to 40 min for a rCBF range around 50 ml/min/100 g.

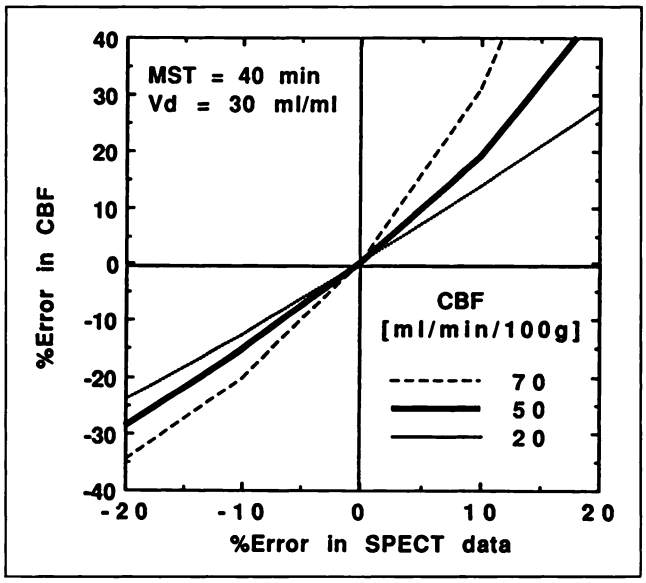

FIGURE 5. Results of a simulation study, demonstrating effects of an error in SPECT data on calculated rCBF value in the IMP ARG method. MST = 40 min post-IMP administration and V_d = 30 ml/ml were assumed. The error propagation factor was approximately 1.5 for the rCBF of 50 ml/min/100 g (i.e., 10% error in the SPECT data corresponds to 15% error in the estimated rCBF values).

putation time for generating the table of $C_t(t)$ (Eq. 4) was less than 0.1 sec, and the table-look-up procedure required 0.1 sec for each tomographic slice (128 × 128 matrix).

Figure 8 shows comparisons of rCBF values obtained by the IMP ARG method (MST = 40 min and V_d = 30 ml/ml) and those by the ^{15}O-water PET method (Group 1 and Group 2, respectively). In Group 2, no significant difference was found between the smoker (n = 4) and nonsmoker (n = 6) groups. Figure 9 shows a comparison of rCBF values calculated by the IMP ARG method with those by the NLLSF analysis for the Group 1. The results of a linear-regression analysis are summarized in Table 4 for various MSTs for the first group. Significant correlations were observed for all MSTs between the present method and the other two methods (the ^{15}O-water PET and the IMP NLLSF methods). The interregional correlation was also found to be significant within individuals, as shown in Table 5. The rCBF values by the IMP ARG method were slightly smaller than those by the ^{15}O-water PET method by a factor of approximately 20% (Fig. 8).

DISCUSSION

IMP has relatively high first-pass extraction fraction in the brain, which is an important requirement for quantitative assessment of rCBF in vivo with use of SPECT (*1,2*). However, it has been reported by several workers that the radioactivity distribution varies after the administration of IMP (*2–12*). This change was seen not only in the absolute radioactivity concentration but also in a relative contrast within the individual (*2,4,5*). The change of the IMP distribution makes application of the conventional microsphere model difficult and of the limited accuracy in the calculation of the quantitative rCBF image from a static brain-IMP map. Kuhl et al. (*2*) explained the time course of the IMP distribution as a phenomenon caused by the clearance (washout) of IMP from the brain, and they first suggested the use of the two-compartment model to describe the kinetics in the brain. Values of rCBF were then calculated according to the NLLSF technique simultaneously with the clearance rate constant (k_2). Validity of this model was also suggested by Greenberg et al. (*6*) and more recently by Yokoi et al. (*10*). This technique, however, has been of limited applicability for clinical use because it

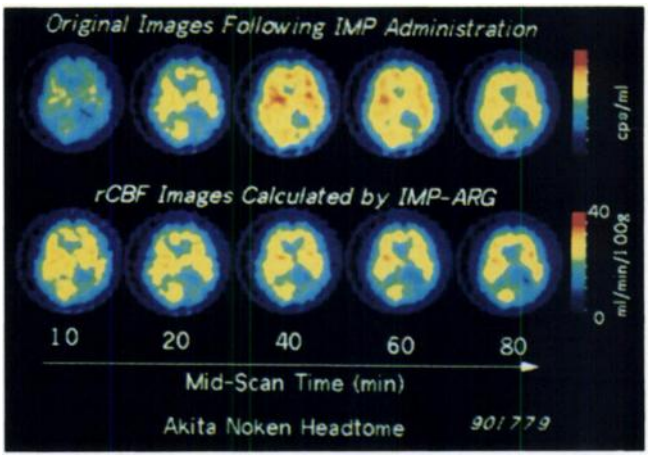

FIGURE 6. Original radioactivity distribution images (upper) and calculated rCBF images (lower) for various MSTs following IMP administration obtained from a patient with chronic cerebral infarction (Group 1). In the original images, both absolute counts and regional distribution were significantly changed because MST was delayed, whereas the calculated rCBF images showed only small differences for all MSTs. The contrast between high- and low-flow areas was higher in the calculated rCBF images than in that of the original IMP images. This improvement is particularly clear at MST greater than 20 min.

TABLE 3
Summary of NLLSF Analysis for Dynamic SPECT Data with Results from Oxygen-15-Water PET and the Present Methods*

	rCBF (ml/min/100 g)	V_d (ml/ml)	No.
NLLSF (IMP)			
Total	29.0 ± 12.0	30.1 ± 7.2	50
Normodensity in x-ray CT	31.3 ± 10.4	31.5 ± 3.0	45
Low density in x-ray CT	8.7 ± 4.2†	10.1 ± 4.9	5
^{15}O-water PET			
Total	34.2 ± 12.8		50
Normodensity in x-ray CT	37.2 ± 9.6		45
Low density in x-ray CT	7.7 ± 5.4†		5
IMP ARG (the present method) MST = 40 min			
Total	25.7 ± 11.4		50
Normodensity in x-ray CT	27.8 ± 10.0		45
Low density in x-ray CT	7.0 ± 3.1		5

*Data are shown for all ROIs (total), regions that showed normodensity and low density on x-ray CT.

†$p < 0.001$ between normodensity and low-density regions.

ARG = autoradiography; MST = midscan time; V_d = volume of distribution.

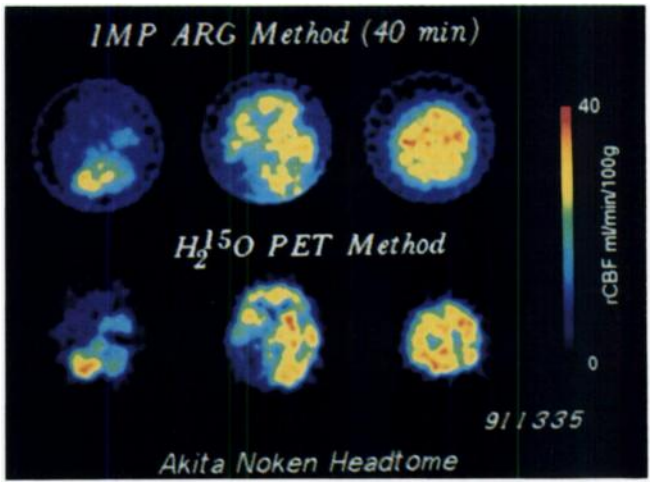

FIGURE 7. Functional rCBF images at three different tomographic slices calculated by the IMP ARG method (upper) and those by ^{15}O-water PET method (lower). Data were obtained from a patient with chronic cerebral infarction (Group 1). The same color scale is used to display these two quantitative rCBF images.

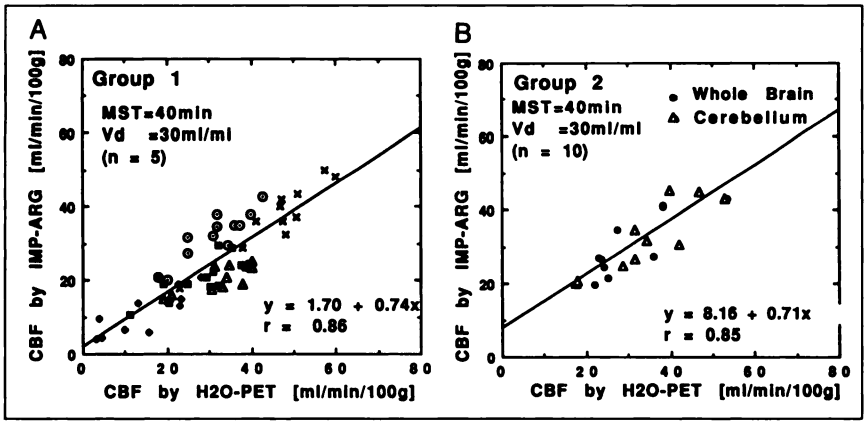

FIGURE 8. Comparison of rCBF values obtained by the IMP ARG method with those by the ^{15}O-water PET method. MST was 40 min, and the whole-blood radioactivity concentration measured at t = 9 min was referred to scale the standard input function. V_d was assumed to be 30 ml/ml. (A) Data were obtained from the first group (n = 5 subjects). Each mark corresponds to a subject. Twelve ROIs were selected in each subject. (B) Data obtained from the second group (n = 10 subjects). Closed circles and open triangles correspond to the whole brain (a region that includes a whole tomographic slice at 40 mm above OM line) and the cerebellum, respectively. Significant correlation was confirmed in both groups between the two methods. Regional correlation was also found to be significant within the subjects in Group 1 (Table 5). The IMP ARG method underestimates rCBF compared with the ^{15}O-water PET method by a factor of approximately 20%.

required dynamic SPECT data acquisition in addition to frequent arterial blood sampling and measurements of lipophilic fraction for each sample, which would be too laborious as a routine clinical tool. An alternative approach was also suggested by Kuhl et al. (*2*), in which the SPECT scan was initiated at an extremely early period post-IMP administration (e.g., less than 5 min) so that the conventional microsphere model may be applied. Limitation of the early data acquisition was, however, associated with the limitation of accuracy in the reconstructed SPECT images for the data being acquired when the radioactivity is varying. It was also shown by Murase et al. (*9*) and Yokoi et al. (*10*) that systematic underestimation could be introduced even with a relatively early SPECT scan (e.g., at 5 min). In addition, a continuous withdraw of the arterial blood was required in this approach, which would not be easy to perform routinely in clinical studies.

This article describes a new method for measuring quantitative images of rCBF from a tomographic image of the IMP distribution taken at an arbitrary time. This technique requires only a single SPECT scan and one blood sample following intravenous administration of IMP. These procedures are significantly easier than those required for the NLLSF or the microsphere techniques. The clearance of IMP from the brain, which becomes an important error source particularly when data are acquired at a delayed period, was taken into account by employing the two-compartment model. The nonlinear relationship between the observed radioactivity concentration (counts in each pixel of the SPECT image) and the rCBF was corrected by assuming the distribution volume of IMP (V_d). Functional maps of rCBF were then calculated from the observed original images by employing the table-look-up algorithm. The image-processing time of this method (including generation of the table and the table-look-up procedure) was rapid and therefore advantageous when this method is applied to clinical studies.

In this article, the generation and use of a standard input function and its calibration by one-point blood sampling were validated, thus obviating the need for frequent (or continuous) arterial blood sampling and measurement of

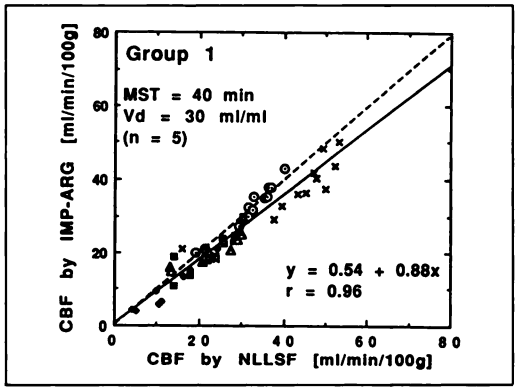

FIGURE 9. Comparison of rCBF values obtained by the IMP ARG method with those by NLLSF analysis. Data were obtained from the first group (n = 5 subjects). Each mark corresponds to each subject. The IMP ARG method used a single SPECT scan data taken at MST = 40 min and a whole-blood radioactivity concentration of one arterial blood sample at 9 min; V_d = 30 ml/ml was assumed. The NLLSF method used all frames of the dynamic SPECT scan data and the individual input function that was obtained from frequent arterial blood sampling and measurements of octanol extraction fractions for each sample. It should be noted that rCBF values were in good agreement between the two methods, which suggests the accuracy of using the standard input function and calibrating it by one blood sample for the rCBF estimates. The solid line denotes the results of the linear-regression analysis. The dashed line denotes the line of identity.

TABLE 4
Results of Linear-Regression Analysis for Various SPECT Scan Times Obtained from Group 1 (n = 5)

SPECT Midscan time	IMP ARG vs. ^{15}O-water PET		IMP ARG vs. IMP NLLSF	
	Regression line	r Value	Regression line	r Value
10	y = 3.01 + 0.59x	0.77	y = 0.96 + 0.78x	0.85
20	y = 1.41 + 0.71x	0.86	y = 0.33 + 0.84x	0.96
30	y = 2.66 + 0.69x	0.86	y = 1.48 + 0.83x	0.95
40	y = 1.69 + 0.74x	0.86	y = 0.54 + 0.88x	0.96
50	y = −0.27 + 0.81x	0.85	y = −1.67 + 0.96x	0.96
60	y = −0.35 + 0.79x	0.83	y = −1.60 + 0.94x	0.93

the lipophilic component for each sample. Errors can be introduced by the interindividual difference of the arterial input function but are minimized by choosing an optimal SPECT MST. It is shown in Figure 4 that the error is minimum (approximately 10% for rCBF = 50 ml/min/100 g) when the SPECT MST was between 20 and 40 min post-IMP administration. The empirical validity of using the standardized input function is also shown in Figure 9, in which rCBF values calculated by use of the standardized input function (the IMP ARG method) agreed well with those by the NLLSF method that employed the individually measured arterial input function. The small dependency of the slope in each patient shown in Figure 9 (Table 5) was probably due to the individual difference of the arterial input function and was found to be small.

The validity of fixing the V_d value was also suggested by a simulation study (Fig. 3). The errors due to ambiguity in the V_d value in each ROI of each subject were relatively small particularly at a low rCBF region, whereas NLLSF analysis demonstrated that V_d values were relatively stable in normal tissue regions (approximately 10% s.d.). It was shown that an error in V_d of 10% caused an error in rCBF of approximately 7% for MST of 30 min at rCBF = 50 ml/min/100 g. Agreement of the calculated rCBF values between the IMP ARG method and NLLSF shown in Figure 9 also empirically suggests the validity of fixation of the V_d value. It should be noted that the data shown in Figure 9 include not only the normal regions but also the infarcted regions as identified by x-ray CT (significant decrease of V_d values was also observed in these regions). The small error in such regions is due to the fact that the rCBF values in regions with reduced V_d were always reduced and that no region showed preserved rCBF when V_d was reduced. Note that the error sensitivity to V_d was small when rCBF was small (Fig. 3).

The present study demonstrated that rCBF values calculated by this technique are constant and independent of the SPECT MST, whereas the radioactivity concentration in the regional brain varied as the SPECT MST was delayed (Fig. 6). It was also demonstrated that the calculated rCBF values were significantly correlated with those obtained by the ^{15}O-water PET technique, although the IMP ARG method provides smaller rCBF values than the ^{15}O-water PET method. Consistency of the IMP ARG method against the two references (i.e., the ^{15}O-water PET and IMP NLLSF methods) was also confirmed within individuals (Table 5). These findings suggest the validity of the present IMP ARG method to measure quantitative rCBF values from a single SPECT scan and one blood sampling.

The magnitude of the total error (accuracy) in the calculated rCBF may be estimated from known sources of errors as follows. The following might be the dominant factors: (1) errors caused by individual difference of the input function, (2) errors resulting from individual difference of V_d value and (3) errors in the original SPECT image.

It was shown in Figure 4 that an approximately ± 10% error was caused by the difference of individual input function for MST of 30 min and rCBF = 50 ml/min/100 g (including the ambiguity of the calibration of the standardized input function). From Figure 3, it can be estimated that variations in true V_d of ± 10% (1 s.d. at the normal density regions on x-ray CT, Table 3) can cause ± 7% error

TABLE 5
Results of Linear-Regression Analyses in Each Subject from Group 1

Subject	IMP ARG vs. ^{15}O-water PET		IMP ARG vs. IMP NLLSF	
	Regression Line	r Value	Regression Line	r Value
1	y = 7.32 + 0.80x	0.90	y = −1.75 + 1.06x	0.97
2	y = 7.38 + 0.40x	0.80	y = 7.38 + 0.41x	0.81
3	y = 3.82 + 0.74x	0.93	y = 2.82 + 0.79x	0.92
4	y = 5.61 + 0.53x	0.80	y = 0.74 + 0.88x	0.89
5	y = 3.13 + 0.55x	0.85	y = −0.49 + 0.85x	0.97

*Midscan time = 40 min and volume of distribution = 30 ml/ml in the IMP ARG method. Number of ROIs was 12 in each subject.

in the calculated rCBF at rCBF = 50 ml/min/100 g. The exact magnitude of the error caused by the inaccurate reconstruction of SPECT data is unknown but can be introduced by nonuniformity of the reconstructed images as a result of inaccurate attenuation correction or scatter, in addition to the statistical noise of the SPECT image. Errors can also be caused by the transient change of the radioactivity change during the SPECT data acquisition. The quantitative SPECT counts can also be affected by the limited spatial resolution (the partial volume effect) and the Compton scatter events in the object. All these factors should affect the accuracy of the rCBF estimates. Application of error propagation rule provides the statistical error in the calculated rCBF values:

$$\sqrt{(\text{error by input})^2 + (\text{error by } V_d)^2 + (\text{error in SPECT})^2}. \quad \text{Eq. 6}$$

If the error in the SPECT data (statistical noise) is neglected, the statistical error in the calculated rCBF values (for a typical condition of MST = 30 min and f = 50 ml/min/100 g) may be calculated as $\sqrt{(10\%)^2 + (7\%)^2} \approx 12\%$. This estimated error should be larger for higher rCBF estimates but would be smaller for the low rCBF estimates.

The most dominant factor to limit the accuracy of the present method is due to the individual difference of the input function (the first factor). This error may therefore be reduced if the standard input function could be defined more precisely, e.g., by dividing patients into different age groups, smoking or nonsmoking groups, or disorders of pulmonary or cardiac functions. Further study should be performed for this.

One of the reasons for the underestimation of rCBF values in the IMP ARG method compared with the ^{15}O-water PET method by a factor of approximately 20% (Fig. 8) was probably due to the limited first-pass extraction fraction (E) of IMP. In this article, E was assumed to be unity. However, it has been reported by Kuhl et al. (*2*) that E was 0.92 and 0.74 for hemispheric rCBF of 0.33 and 0.66 ml/min/g, respectively. Other investigators (*24*) also reported the permeability-surface area (PS) product for IMP to be 93.4 ml/100 g/min; hence, the Renkin-Crone equation ($E = 1 - e^{-PS/f}$) yields the first-pass extraction fraction to be approximately 0.85 at f = 50 ml/min/100 g (*25,26*). Another reason for the systematic underestimation of rCBF may be due to the poorer spatial resolution of the SPECT scanner compared with the PET scanner that was employed. The limited spatial resolution causes a systematic underestimation in measured radioactivity concentration in the gray matter region and a cross contamination between the gray and white matter regions. Both these factors are expected to cause a systematic underestimation in the calculated rCBF values. The exact magnitude of the underestimation is, however, unknown and most likely patient and ROI dependent. It should also be noted that no scatter correction method was applied to the SPECT data. Significant offset in low rCBF regions caused by the scatter might be included in the SPECT images, which might also explain the declined slope in Figure 8.

Poorer correlation was observed in the comparison of the IMP ARG versus the ^{15}O-water PET methods (Fig. 8) compared with that against the NLLSF method (Fig. 9). Possible explanations for this are (1) limited reproducibility of selecting ROIs of the same region but on different tomographic images, (2) different in-plane and axial spatial resolution between the SPECT and PET scanners and (3) errors in the reference (^{15}O-water PET) method.

The blood sample for calibrating the standard input function was obtained from the arterial line in this study. The time of the blood sample for calibrating the standard input function was determined so as to minimize the difference of integration under the area of the calculated and the true input functions. It might be possible to replace arterial blood sampling by venous blood sampling, which would be a great advantage for using this method in clinical studies. Arterialized venous sampling, as frequently performed in PET studies for FDG and other tracers, or sampling from the peripheral vein (such as dorsal metacarpal vein rather than the antecubital vein) might be suggested. The optimal blood sampling time for venous blood sampling to minimize the calibration error might be slightly later than that determined for arterial blood sampling because of a time shift and distortion (dispersion) of the blood time-activity curve. Further study should be performed to define the optimal calibration time for the venous blood sampling.

The authors previously reported the importance of an accurate determination of the arterial input function for a quantitative measurement of rCBF by use of ^{15}O-water and PET (*20–22*). Only a small delay or dispersion, which can occur in arterial lines, can introduce a large error in the rCBF estimates, and careful corrections were required for these. Although the model for IMP is equivalent to that for ^{15}O-water (two-compartment model), the present study suggested that the IMP study does not require such attention. It has been demonstrated that use of the standardized input function is allowed. With an optimized SPECT scan time, the errors caused by individual differences of the input function were found to be small, and quantitative rCBF values can be obtained with an acceptable accuracy (± 10%). This difference between the IMP and ^{15}O-water studies is probably due to differences in the V_d value (approximately unity for the ^{15}O-water compared with approximately 30 ml/ml for IMP). The larger V_d value for IMP allows the SPECT scan time to be delayed compared with that in the ^{15}O-water study. This makes the convolution integral of Equation 1 insensitive to individual differences (delay and dispersion) in the shape of the input function. A difference in the shape of the input function around the peak does not affect the integration of the input function.

In this study, the standard input function was obtained following a constant infusion of IMP over 1 min. It might

therefore be important to follow this protocol for applying this standard input function to the clinical study. Values of the table (left side of Equation 4) are unlikely to change very much, but the calibration factor, which is determined from the standard whole-blood radioactivity curve, may be affected. Slightly delayed blood sampling should be recommended if the infusion protocol is modified.

The V_d value, which is fixed in the IMP ARG method, is defined as the influx-to-outflux rate constants (K_2/k_2) and can be expressed as $V_d = \rho \cdot \lambda$, as shown in Equation 3. In this study, the V_d value was obtained from the dynamic SPECT study on the subjects belonging to Group 1. Because ρ indicates the proportion of the tissue within the volume of ROI (see Eq. 1 and 4), the V_d value would be dependent on the intrinsic performance of the SPECT scanner, such as its spatial resolution and scatter component. The V_d value may therefore have to be determined for each SPECT scanner and for each reconstruction algorithm. It should also be noted that, in this study, the patients who underwent the dynamic SPECT study had cerebral infarctions and severe neurologic deficits. The obtained V_d value may therefore be smaller than the true normal value (even though the values were calculated for the normodensity regions). Further study would be suggested to measure the V_d value for normal subjects.

There is not a clear physiologic justification for the two-compartment model for describing the IMP kinetic characteristics in the brain. However, empirical validity has been demonstrated previously by Yokoi et al. (*10*) using a unique approach to analyze the dynamic IMP data based on a graphic plot which proved empirically that the IMP followed the two-compartment model until 180 min after IMP administration. A systematic error can be caused by tissue heterogeneity, but the magnitude of the error was found to be small (less than 5%) in the calculated rCBF value (*10*).

CONCLUSIONS

A method was developed to measure quantitative rCBF from a single SPECT scan and single blood sampling in which the clearance of IMP from the brain was taken into account by employing the two-compartment model. Use of the standard input function avoided frequent arterial blood sampling and separation of the lipophilic fraction. The distribution volume of IMP (V_d) was determined prior to this study (V_d = 30 ml/ml). This technique yielded rCBF values, which agreed with those measured by the ^{15}O-water PET method. Obtained rCBF values also agreed with those from conventional NLLSF analysis that individually measured the arterial input function. This study also suggested that the SPECT scan should be performed at 20 to 40 min and the blood sample should be taken at 9 min after IMP administration to provide the most accurate rCBF value.

ACKNOWLEDGMENTS

The authors thank Mr. Stefan Eberl, MSc, from Royal Prince Alfred Hospital (Sydney, Australia) for invaluable discussion and advice in preparing the manuscript. We are indebted to the staff of Research Institute for Brain and Blood Vessels, Akita; in particular, Yasuo Aizawa, Takenori Hachiya and Yasuaki Shoji, for handling the SPECT and PET scanners. This work was supported by a 1990 grant from the Japan Heart Foundation.

REFERENCES

1. Winchell HS, Horst WD, Braun L, et al. N-isopropyl [^{123}I]p-iodoamphetamine: single-pass brain uptake and washout; binding to brain synaptosomes; and localization in dog and monkey brain. *J Nucl Med* 1980;21:947–952.
2. Kuhl DE, Barrio JR, Huang SC, et al. Quantifying local cerebral blood flow by N-isopropyl-p [I-123] iodoamphetamine (IMP) tomography. *J Nucl Med* 1982;23:196–203.
3. Podreka I, Baumgartner C, Suess E, et al. Quantification of regional cerebral blood flow with IMP-SPECT: reproducibility and clinical relevance of flow values. *Stroke* 1989;20:183–191.
4. Creutzig H, Schober O, Gielow P, et al. Cerebral dynamics of N-isopropyl-^{123}I)p-iodoamphetamine. *J Nucl Med* 1986;27:178–183.
5. Nishizawa S, Tanada S, Yonekura Y, et al. Regional dynamics of N-isopropyl-(^{123}I)p-iodoamphetamine in human brain. *J Nucl Med* 1989;30:150–156.
6. Greenberg JH, Kushner M, Rango M, Alavi A, Reivich M. Validation studies of iodine-123-iodoamphetamine as a cerebral blood flow tracer using emission tomography. *J Nucl Med* 1990;31:1364–1369.
7. Matsuda H, Higashi S, Tsuji S. A new noninvasive quantitative assessment of cerebral blood flow using N-isopropyl-(iodine 123)p-iodoamphetamine. *Am J Physiol Imaging* 1987;2:49–55.
8. Takeshita G, Maeda H, Nakane K, et al. Quantitative measurement of regional cerebral blood flow using N-isopropyl-(iodine-123)p-iodoamphetamine and single-photon emission computed tomography. *J Nucl Med* 1992; 33:1741–1749.
9. Murase K, Tanada S, Mogami H, et al. Validity of microsphere model in cerebral blood flow measurement using N-isopropyl-p-(I-123) iodoamphetamine. *Med Phys* 1990;17:79–83.
10. Yokoi T, Iida H, Itoh H, Kanno I. A new graphic plot analysis for cerebral blood flow and partition coefficient with iodine-123-iodoamphetamine and dynamic SPECT validation studies using oxygen-15-water and PET. *J Nucl Med* 1993;34:498–505.
11. Itoh H, Iida H, Bloomfield PM, et al. A technique for a rapid imaging of rCBF and partition coefficient using dynamic SPECT and I-123-amphetamine (IMP). *J Nucl Med* 1992;33(suppl):911.
12. Iida H, Itoh H, Munaka M, et al. A clinical method to quantitate CBF using a rotating gamma camera and I-123amphetamine (IMP) with one blood sampling. *Eur J Nucl Med* 1994;21:1072–1084.
13. Kanno I, Uemura K, Miura S, Miura Y. Headtome: a hybrid emission tomography for single photon and positron emission imaging of the brain. *J Comput Assist Tomogr* 1981;5:216–226.
14. Hirose Y, Ikeda Y, Higashi Y, et al. A hybrid emission CT-Headtome II. *IEEE Trans Nucl Sci* 1982;NS-29:520–523.
15. Tanaka E. Quantitative image reconstruction with weighted backprojection for single emission computed tomography. *J Comput Assist Tomogr* 1983; 7:692–700.
16. Iida H, Miura S, Kanno I, et al. Design and evaluation of Headtome-IV, a whole-body positron emission tomograph. *IEEE Trans Nucl Sci* 1989;NS-36:1006–1110.
17. Herscovitch P, Markham J, Raichle ME. Brain blood flow measured with intravenous $H_2^{15}O$. I. Theory and error analysis. *J Nucl Med* 1983;24:782–789.
18. Raichle ME, Martin WR, Herscovitch P, Markham J. Brain blood flow measured with intravenous $H_2^{15}O$. II. Implementation and validation. *J Nucl Med* 1983;24:790–798.
19. Kanno I, Iida H, Miura S, et al. A system for cerebral blood flow measurement using an $H_2^{15}O$ autoradiographic method and positron emission tomography. *J Cereb Blood Flow Metab* 1987;7:143–153.
20. Iida H, Kanno I, Miura S, et al. Error analysis of a quantitative cerebral blood flow measurement using $H_2^{15}O$ autoradiography and positron emission tomography: with respect to the dispersion of the input function. *J Cereb Blood Flow Metab* 1986;6:536–545.

21. Iida H, Higano S, Tomura N, et al. Evaluation of regional difference of tracer appearance time in cerebral tissues using [^{15}O]water and dynamic positron emission tomography. *J Cereb Blood Flow Metab* 1988;8:285–288.
22. Iida H, Kanno I, Miura S, et al. A determination of regional brain/blood partition coefficient of water using dynamic positron emission tomography. *J. Cereb Blood Flow Metals* 1989;9:874–885.
23. Iida H, Kanno I, Miura S. Rapid measurement of cerebral blood flow with positron emission tomography. *CIBA Found Symp* 1992;163:23–42.
24. Renkin EM. Transport of potassium-42 from blood to tissue in isolated mammalian skeletal muscles. *Am J Physiol* 1959;197:1205–1210.
25. Crone C. The permeability of capillaries in various organs as determined by use of the indicator diffusion method. *Acta Physiol Scand* 1963;58:292–305.
26. Huang SC, Mahoney DK, Phelps ME. Quantitation in positron emission tomography: 8. Effects of nonlinear parameter estimation on functional images. *J Comput Assist Tomogr* 1987;11:314–325.
27. Murase K, Tanada S, Inoue T, et al. Measurement of the blood-brain barrier permeability of I-123 IMP, Tc-99m HMPAO and Tc-99m ECD in the human brain using compartment model analysis and dynamic SPECT. *J Nucl Med* 1991;32(suppl):911.